water

MDPI

Article

Modeling Rainwater Harvesting and Storage Dynamics of Rural Impoundments in Dry Chaco Rangelands

Marcos Javier Niborski [1,2,*], Osvaldo Antonio Martin [3], Francisco Murray [4], Esteban Gabriel Jobbágy [1], Marcelo Daniel Nosetto [1,5], Ricardo Andrés Paez [1] and Patricio Nicolás Magliano [1,6]

1 Grupo de Estudios Ambientales-IMASL, Universidad Nacional de San Luis (UNSL) y CONICET, San Luis D5700HHW, Argentina; jobbagy@gmail.com (E.G.J.); marcelo.nosetto@gmail.com (M.D.N.); ricardo.paez1@gmail.com (R.A.P.); pnmagliano@gmail.com (P.N.M.)
2 Cátedra de Manejo y Conservación de Suelos, Facultad de Agronomía, Universidad de Buenos Aires (UBA), Buenos Aires C1417DSE, Argentina
3 IMASL, Universidad Nacional de San Luis (UNSL) y CONICET, San Luis D5700HHW, Argentina; omarti@unsl.edu.ar
4 INTA, AER San Luis, San Luis D5700HHW, Argentina; murrayfrancisco@inta.gob.ar
5 Cátedra de Climatología, Facultad de Ciencias Agropecuarias, Universidad Nacional de Entre Ríos (UNER), Concepción del Uruguay E3260FIB, Argentina
6 Departamento de Biología, Facultad de Química, Bioquímica y Farmacia, Universidad Nacional de San Luis (UNSL), San Luis D5700HHW, Argentina
* Correspondence: marcosniborski@gmail.com

Abstract: Transporting water to supply livestock is one of the great challenges of the drylands. Ranchers usually make impoundments, filled by runoff, to access freshwater for cattle supply in flat rangelands. The aim of this study was to understand rainfall-runoff generation and water storage temporal dynamics of impoundments in the Dry Chaco rangelands (Argentina). Thus, we instrumented six impoundments over three consecutive years and analyzed water storage data by developing a probabilistic model. For all impoundments, the rainfall event size thresholds to generate runoff presented values between 15 and 33 mm. Once they reached this threshold, the water gain response slopes presented values between 19 and 99 m^3 mm^{-1}. Loss patterns of water storage were described by exponential or linear functions. The predicted water storage dynamics presented high accuracy with the observed time series for all impoundments (RMSD between 380 and 1320 m^3). The model only needs daily rainfall and air temperature to be run, making it easy to be used by scientists, ranchers, or local decision makers. It may be used to explore the hydrological functioning of small and seasonal water bodies of different sites of the world exposed to drought episodes caused by high climate variability and/or climate change.

Keywords: atmospheric demand; arid; dams; saturated overland flow; precipitation; water balance; Bayes

Citation: Niborski, M.J.; Martin, O.A.; Murray, F.; Jobbágy, E.G.; Nosetto, M.D.; Paez, R.A.; Magliano, P.N. Modeling Rainwater Harvesting and Storage Dynamics of Rural Impoundments in Dry Chaco Rangelands. *Water* **2023**, *15*, 2353. https://doi.org/10.3390/w15132353

Academic Editors: Saeid Mehdizadeh and Farshad Ahmadi

Received: 23 May 2023
Revised: 13 June 2023
Accepted: 15 June 2023
Published: 25 June 2023

1. Introduction

Drylands represent 40% of the global land and sustain a major fraction of extensive wild and domestic livestock of the world [1–3]. The low rainfall input, usually concentrated in a few months of the year, is the key driver of the net primary productivity that sustains domestic livestock production systems (i.e., cattle production in rangelands) [4–7]. Some rangeland areas exclusively depend on local rainfall inputs as the only option to access freshwater through rainwater harvesting techniques [8,9]. That means that local rainfall must provide enough water for both grass production and freshwater for cattle [10,11]. Thus, understanding the relation between rainfall-runoff generation and hydrological functioning of rural rainwater harvesting systems is critical, especially considering both the natural high climate variability [7,12] and the climate change trends predicted for these areas [13,14].

Since thousands of years ago, local communities of drylands have developed rainwater harvesting systems to obtain freshwater from the small fraction of the landscape that generates runoff [15,16]. Although runoff represents less than 5% of annual rainfall in drylands [6,17,18], it has a key role at collecting freshwater, making cattle production possible in these areas [19–21]. For example, cattle production in the South American Dry Chaco rangelands (i.e., Arid Chaco) exclusively relies on rainwater harvesting systems made by local communities and ranchers. The need for rainwater harvesting systems is the result of the combination of (i) low rainfall inputs (e.g., ~400 mm y^{-1}), (ii) high potential evapotranspiration (e.g., ~1500 mm y^{-1}), (iii) absence of permanent surface water bodies (e.g., lagoons, lakes, or rivers), and (iv) the very deep water tables (e.g., ~100 m deep). The most widespread rainwater harvesting systems in this region are impoundments with a typical size of 100 × 50 × 2 m, built by the ranchers with road machinery [22–24]. On average for the ~10 Mha of Dry Chaco rangelands, there is one impoundment every 1230 ha, with hotspots of one impoundment every 300 ha (i.e., Belgrano department, San Luis province) [25].

In Dry Chaco rangelands, as in other seasonal drylands of the world, rainfall is highly concentrated in a few months of the year. In this system, the delay in the occurrence of the first rainfall events of the year or the shortening of the wet season may have a critical impact on cattle production, as well as on human well-being. In addition, droughts, defined as years with rainfall input with less than 75% of the historical mean rainfall of a site, are recurrent in this region [26] and may be exacerbated in a climate change context. To prevent the lack of water during dry seasons or drought periods, the cities of this region are supplied by big reservoirs, or dikes, that collect water from the mountains located several kilometers away [27–29]. However, in rangelands or rural sites, where the water supply is only guaranteed by the in situ rainwater harvesting systems (i.e., impoundments), extreme droughts may force ranchers to sell their cattle in a hurry and usually at unfavorable prices. Even in some extreme cases, ranchers and rural people must abandon the territory because of water scarcity. Therefore, monitoring water resources in Dry Chaco rangelands is very necessary to anticipate events of water shortage, and to mitigate the effects of droughts. For example, it would be useful to be able to predict the water storage of impoundments at the end of the wet season in order to estimate the probability that the stored water will last until the beginning of the following wet season.

Despite their relevance to cattle production, there is little scientific evidence of the hydrological functioning of rainwater harvesting systems. Further, there is no previous work in the Dry Chaco describing the hydrological functioning of rainwater harvesting systems, or models to predict their water storage and supply abilities. In this study, we developed a hydrometeorological data-based temporal model to explore the hydrological functioning of rainwater harvesting systems of Dry Chaco rangelands. More specifically, we first characterized the temporal dynamic of water stored into impoundments together with the atmospheric conditions, then we developed an empirical model with a physical basis that captured the temporal hydrological functioning of each impoundment at the daily scale. To do this, we first instrumented six impoundments with water level sensors and rain gauges during three consecutive years, then we used a Bayesian approach to develop models able to predict different hydrological scenarios.

2. Materials and Methods

2.1. Study Area

The study area is located in the Arid Chaco (Dry Chaco rangelands) that covers ~10 Mha of the southwest of the Chaco ecoregion, and represents the most arid fraction of it [30]. Valleys and foothills, within large sedimentary plains of reddish materials that are sometimes salinized, define a system of arreic basins, with small, intermittent and seasonal water courses, defined by their low slope and high sediment load [30–32]. Groundwater is deeper than 60 m in almost the entire region, therefore, it does not exert direct influence on the vegetation. The vegetation matrix is composed by xerophytic forests of *Prosopis*

flexuosa and *Aspidosperma quebracho-blanco* trees, and *Larrea divaricata* shrubs, with native grasslands of *Digitaria californica*, *Trichloris crinita*, *Aristida mendocina*, *Setaria cordobensis* and *Pappophorum caespitosum* dominating the herbaceous stratum [31]. Mean annual rainfall is ~400 mm, concentrated in the spring-summer season [26]. The main economic activity is the extensive cattle production, based on grazing and foraging the native dry forests. In the last 30 years, the ~30% of the dry forests have been replaced by subtropical pastures (mainly *Cenchrus ciliaris*) through traditional deforestation or roller-chopper techniques, in order to increase the cattle production [33–35].

Field measurements took place between 1 May 2019 and 2 September 2022 in a 10,000 ha cattle ranch, located in the northwest of the province of San Luis (−33.05° S, −66.81° W; Figure 1). This establishment, named San Agustin, has six permanently active impoundments (Figure 1). At each impoundment, the water level, rainfall and air temperature were measured. Impoundments are exclusively filled by surface runoff and emptied by evaporation, infiltration, and cattle consumption, with the animals directly entering impoundments to drink water. In general, there is some equidistance between impoundments related to the cattle's capacity to move between water sources and grazing sites. The selection of places where the impoundments are built is usually decided by ranchers and local rural workers, based on their empirical knowledge. They identify both the areas of the landscape that generate runoff, called "water avenues" by them, and the best position in the landscape to minimize sediment loading with incoming water. That is why most of the impoundments were named after the people who chose the place or built it. Although the six impoundments were built and managed in a similar way, the number of measurement sites and their distribution has an adequate representation of the spatial variability of this region [25].

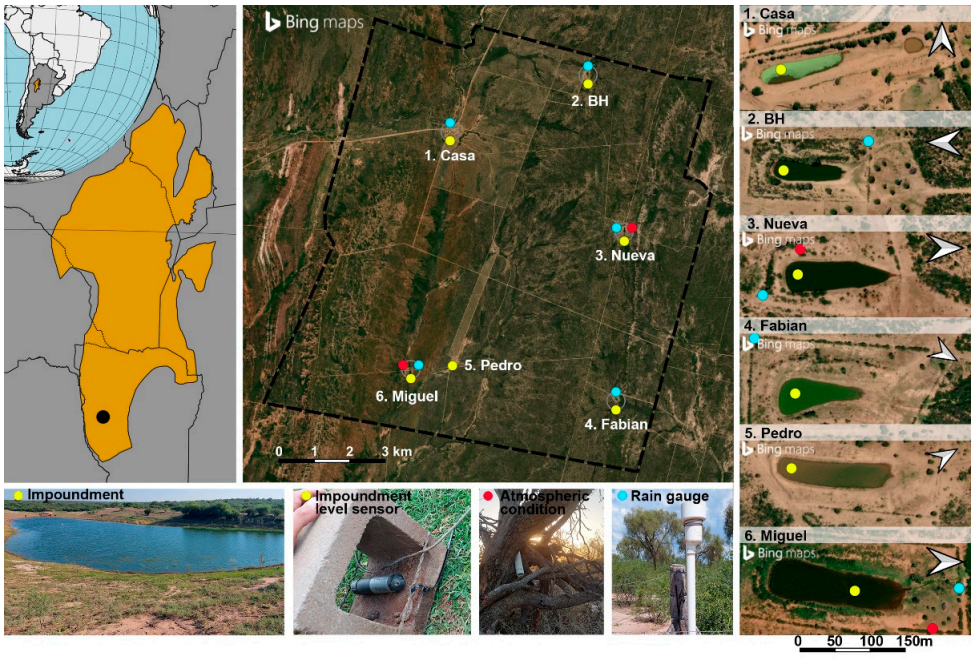

Figure 1. Study area and experimental design of measurements. (**Left**): Arid Chaco (orange polygon) in the northwest of San Luis province of Argentina. (**Center**): San Agustin establishment (black dashed boundary line) where impoundments water level (yellow dots), air temperature (red dots) and rainfall (light blue dots) were measured. Some illustrative photos are presented at the bottom showing, from the left to the right, a full-filled impoundment, a water level sensor, a temperature and atmospheric pressure sensor, and a rain gauge. (**Right**): high-resolution satellite imagery provided by Bing server, zoomed to each impoundment with the location of the sensors.

2.2. Field Measurements and Data Processing

While water level measurements were made in six impoundments, rainfall was measured in five locations, because two impoundments were very close to each other. Air temperature and atmospheric pressure were measured in two impoundments (Figure 1). All data (water level and meteorological variables) were recorded with transducer sensors with incorporate dataloggers (ONSET HOBO U20L-04). All measurements (water level, rainfall, and air temperature) were recorded every 15 min. The 15 min data of water level and air temperature were averaged to obtain daily data, in order to decrease temporal errors. Thus, daily data were composed by the mean of 96 values representing a confidence value. Rainfall was calculated as the differences between consecutive 15 min data, summarized at each day. Water level sensors were located in the deepest point of the six impoundments. Rainfall was measured by installing the water-level sensors into cylindrical pipes. We considered one rainfall event a day, or consecutive days, with data equal or higher than 1 mm. Two additional sensors were located under atmospheric conditions to register air temperature and atmospheric pressure. Water level values were obtained as the difference between the inside water sensors and the air-exposed ones in order to compensate for the atmospheric pressure. Thus, as all data (water level, rainfall, atmospheric pressure, and air temperature) was obtained with the same sensor model, the experimental error of measurements was negligible. In addition, all sensors were temporally synchronized, and data were downloaded every six months using the same notebook.

To convert the daily water column (cm) of impoundments into daily water volume (m^3), we made a bathymetry of each impoundment. To do this, we used high-resolution PlanetScope imagery (3 m, Dove satellite constellation with PS2.SD and PSB.SD sensors) provided by Planet (Image© 2019–2022 Planet Labs PBC). At each impoundment, we chose 7 images exposed to different water level depths (<50 cm, 50–100 cm, 100–150 cm, 150–200 cm, 200–250 cm, 250–300 cm and >300 cm). Then, we drew up the water surface boundary lines from the images and we assigned a level value to each, to create a digital elevation model with QGIS complements. Finally, we related imagery water surface data with water level data provided by in situ water level sensors to convert water depth (cm) in water volume (m^3).

2.3. Water Storage Model Development

We built a model to predict the state (impoundment storage) considering the typical conditions of Dry Chaco rangelands, or similar dry and flat systems, described in previous works. More specifically, we assumed that (i) impoundments are filled only from surface runoff events caused by local rainfall events [10,19,25], (ii) not all rainfall events generate water gains into impoundments because there is a threshold to activate runoff processes [22,36,37], (iii) the magnitude of the water gains are proportionally related with the rainfall event size [38,39], (iv) the water volume loss rate is higher when the stored volume is greater [10,19–21], and (v) this flow affected by the atmospheric demand [20,21]. Based on these conditions, the following model was proposed:

$$y_i = y_{i-1}e^{(-\lambda)} - T_i\gamma + r\beta 1_{((r_i+r_{i-1})>\tau)} \quad (1)$$

where, y_i represents the water storage of the impoundments at time i. The first two terms estimate the water losses. The first depends on the previous day water storage (y_{i-1}) that is negatively affected by the exponential of λ. The second is linearly determined with the daily mean air temperature (T_i) as a proxy of the evaporation flux; the strength of the relationship is controlled by the γ coefficient. The last term represents the water gain that was estimated as the product between the rain event size (r) and the water gain response (β) if condition 1 is met that the rainfall event size exceeds the threshold ($(r_i + r_{i-1}) > \tau$), else (i.e., rainfall event size is lower than runoff generation threshold) the whole term become 0. In case the event lasted more than one day, the rain event size was considered as the sum of the present and previous day ($r_i + r_{i-1}$).

Equation (1) has four unknown parameters: λ, γ, β and τ. In order to estimate them, we assumed a probabilistic model where Equation (1) represents the mean of a truncated normal distribution, with a lower bound of 0, and unknown standard deviation. We build the model using PyMC [40,41], assuming weakly informative half normal priors for all the parameters. We used ArviZ [42] for the analysis of the Bayesian models. The input variables in the model were the initial storage (y_0, m^3), the daily rainfall (r_i, mm), and air temperature (T_i, K) time series. The models were sampled using the Sequential Monte Carlo sampler from PyMC with four 4 independent chains, each of 3000 particles. The Rhat (potential scale reduction factor) was lower than 1.01 in all cases. Rank plots also indicated a good quality of the Sequential Monte Carlo samples.

To validate our model, we performed a posterior predictive check [43–46] by comparing empirical cumulative distribution function of the observed and predicted volumes for each of the six impoundments. We also computed the root mean square deviation (RMSD) between observed and predicted volumes.

3. Results

3.1. Temporal Dynamic Patterns

Water storage in impoundments showed a seasonal pattern with maximum values in February and March (summer wet season) and minimum values in October and November (winter dry season; Figure 2). The maximum storage period presented a one-month delay regarding the rainfall peaks. The emptiest period took place at the end of the austral spring, when the atmospheric demand started rising and the rainfall season did not yet start (Figure 2). December and January are the most variable months in terms of water storage. This variability is consequent with the variability in rainfall inputs of these months between years. We only found four months in which all six impoundments had some water (from January to April).

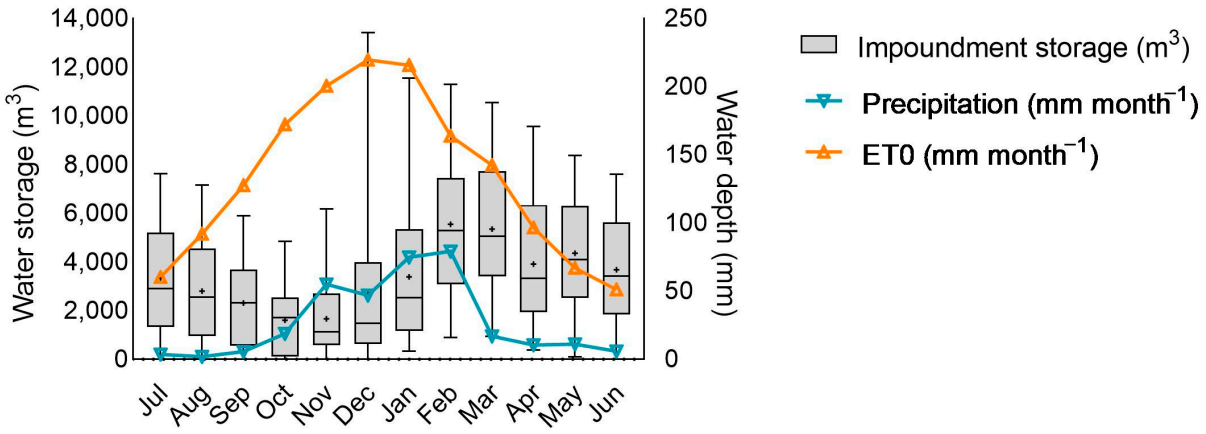

Figure 2. Monthly water storage of impoundments (boxes and whiskers), rainfall (light blue line) and reference evapotranspiration (ET0), standardized by ASCE Penman–Montieth method (orange line). Boxes represent the 25th percentile, median, and 75th percentile, the + symbol represents the mean, and the whiskers represent the 5th and 95th percentiles. Rainfall data correspond to the monthly mean value of the three years' data of the rain gauges installed at the field. ET0 data corresponds to the last 50 years time series of the Terra Climate [47], available in Google Earth engine's collections, from the 4638.3 m pixel where the essay is located.

On average, for the three years, the annual mean rainfall was 389 mm, showing a strong seasonality. A total of 91% of rainfall was concentrated in six months (between October and March) and 64% in three months (between December and February). The maximum number of rainfall events registered per year was between 36 and 48. A total of 10% of them presented sizes larger than 24.5 mm, the highest rainfall event being 114.5 mm depth (Table A1). The three impoundments with greater water gains were Miguel, followed

by Pedro and Nueva (see below), while the impoundments that were never emptied throughout the entire period were Nueva, Fabian and BH (Table A1).

3.2. Storage Modeling

The probabilistic model, when applied to the six different datasets (impoundments) correctly captured their daily variability of water storage. The values of τ threshold (i.e., minimum rainfall event size to generate water gains into the impoundment) were similar for the six impoundments, ranging between 24 and 27 mm for BH, Nueva, Casa, and Pedro, while Fabian and Miguel had the lowest (15 mm) and the highest (33 mm) values, respectively (Table 1). The slopes of the linear water gain responses (β) presented large differences between impoundments. The highest value was found in Miguel (99 m^3 mm^{-1}) and the lowest in BH (19 m^3 mm^{-1}) (Table 1). Finally, the decreasing water storage rate was controlled by an exponential function (as the lower values of λ shows) in Pedro and Miguel, and by a linear function in the other four impoundments (Casa, BH, Nueva, Fabian), because of the higher values of λ that make the term $y_{i-1}e^{(-\lambda)}$ almost negligible. The γ coefficient, which represents the effect of air temperature, was highest in Fabian (0.130 m^3 K^{-1}), while the rest of the impoundments showed lower mean values of between 0.045 and 0.099 m^3 K^{-1} (Table 1).

Table 1. The impoundment's model parameters. The values represent the means of the predicted parameters for each impoundment.

Impoundment	Gain		Loss	
	τ (mm)	**β (m^3 mm^{-1})**	**γ (m^3 K^{-1})**	**λ**
Casa	26	29	0.099	22
BH	24	19	0.045	26
Nueva	26	38	0.087	24
Fabian	15	44	0.130	24
Pedro	27	59	0.079	6
Miguel	33	99	0.089	5

Impoundments showed a positive relation between the rainfall event size threshold and their response to those events, except for Fabian (Figure 3). Thus, impoundments with high rainfall event size threshold (τ) can compensate this aspect with high water gain responses (β). In the case of water loss parameters, the λ values showed two different situations. On the one hand, in four of the six impoundments, the loss rate was not affected by the previous day's storage, but they presented differences in sensitivity to the air temperature changes. On the other hand, in the rest two of the impoundments, the water loss was mostly explained by the exponential decline, which depends on the previous day's storage. It is worth mentioning that BH has the lowest water loss rate by the combination of low γ and high λ. Nevertheless, trying to exemplify the different weight of each loss parameter for a day with mean temperature of 300 K, it expected loss is 39 m^3 in Fabian and 26.7 m^3 in Miguel for the air temperature dependent term only, but if we consider the loss associated with the previous volume, supposing a previous storage of 3300 m^3 in both impoundments, this volume-dependent term increases the daily loss in Miguel by 22 m^3, while in Fabian it is null.

The posterior predictive checking showed high accuracy between the distribution of the observed and predicted values for the six impoundments (Figure 4). Water storage was characterized as a function of water volume along the entire dataset. Casa and Pedro presented some underestimations at low levels of water storage (less than 1000 m^3), while BH and Fabian presented some overestimations at these water storage levels. For water storage values higher than 1000 m^3, all models presented high performance.

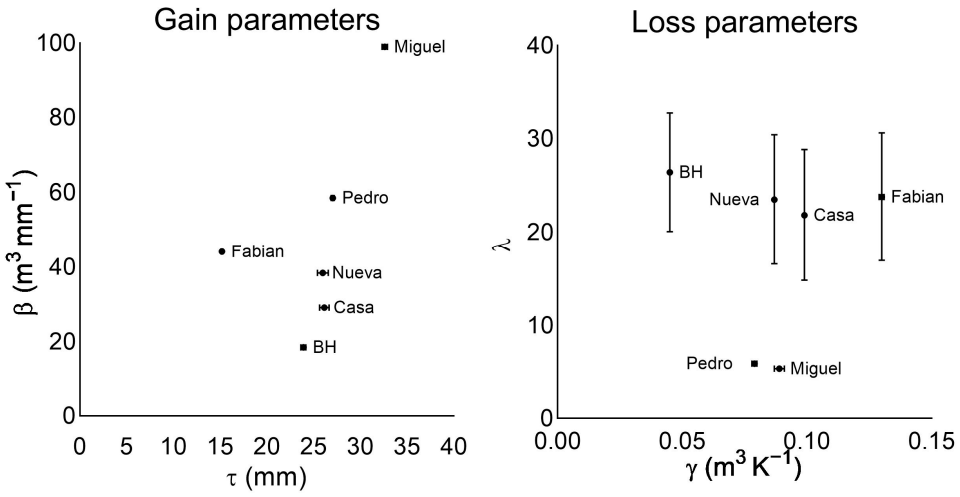

Figure 3. Scatter diagrams of the model's parameters, left. Water gain parameters: impoundment's water gain response (β) versus rainfall event size threshold (τ), right. Water loss parameters: exponential coefficient (λ) versus air temperature coefficient (γ). In both panels, the black dot represents the mean and the whiskers represent the standard deviation for each parameter.

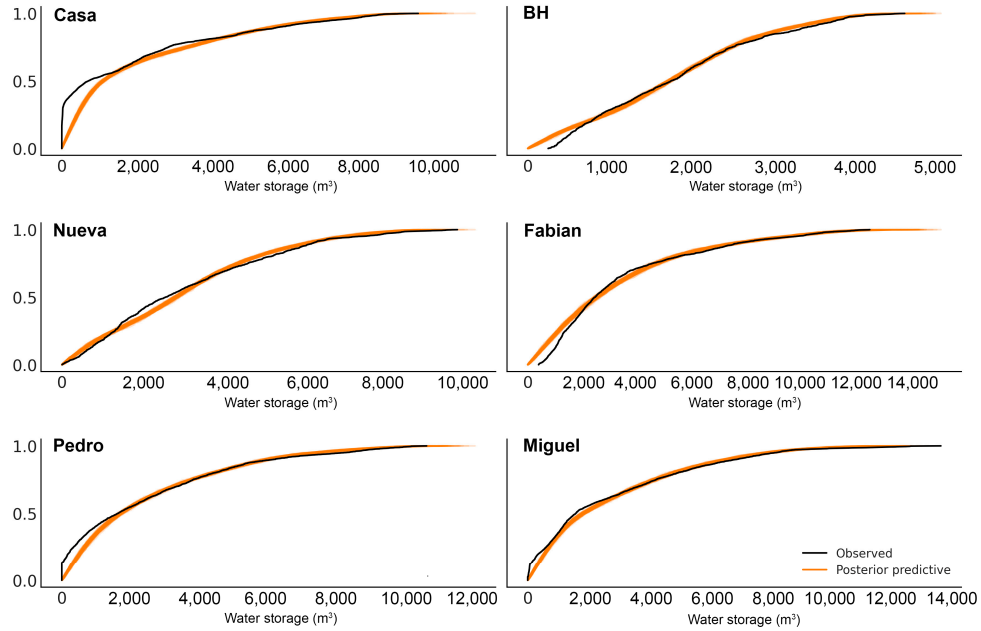

Figure 4. Posterior predictive check showing the accumulated frequency along storage volume increasing values, comparing the observed data (black line) with the posterior predictive (orange lines) for each impoundment.

The predicted water storage dynamics presented high accuracy with the observed time series for all impoundments (Figure 5). In general terms, the maximum and minimum annual storage were represented by the models, and practically all the observed data were included in the predicted bands. BH had the highest accuracy (RMSD = 380.03 m^3) and the narrowest band, while Fabian presented the opposite pattern (RMSD = 1320.54 m^3). Most of the underestimations of the predicted mean took place in Nueva and Fabian when they were emptying in a low storage state due to their high λ. Thus, the emptying process tends to be mostly linear, instead of exponential, as it occurs in the observed values. Instead, the storage's overestimations of the model were associated with large, predicted water gain responses of small rainfall events, and/or when the impoundments were completely empty (Figure 5).

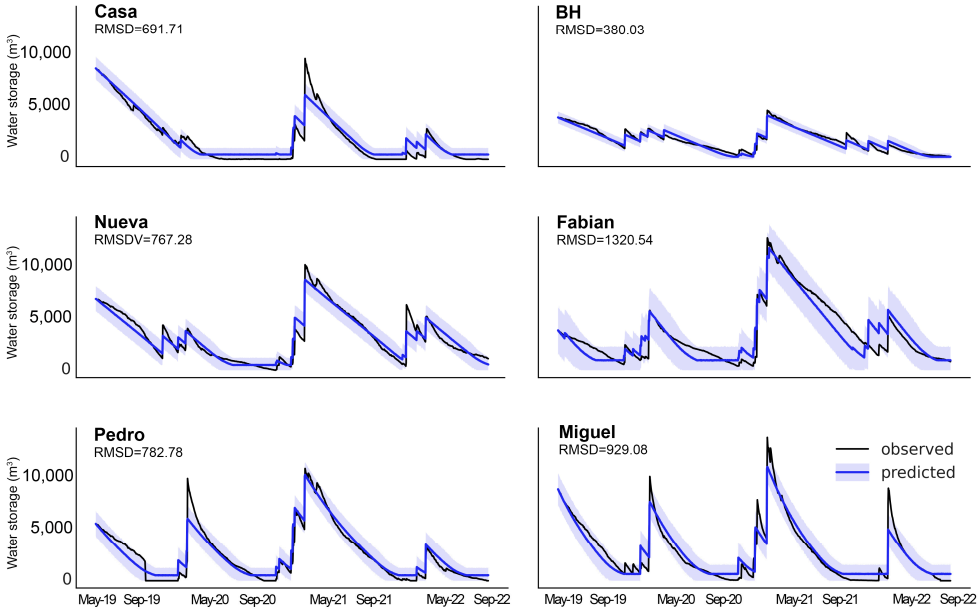

Figure 5. Impoundment water storage modeling results. Each panel shows the root mean square deviation (RMSD) between observed and predicted values, the observed storage temporal series (full black line), the predicted mean values (full blue lines) and the predicted confidence bands (blue shadow) of daily water storage volume (m^3) for the 1220 days that took place between 1 May 2019 and 2 September 2022.

4. Discussion

Understanding rainwater harvesting processes represents a critical issue to enhance livestock production in drylands. Based on long-term high-quality field data series and on a biophysical characterization of the system, we developed a physical model able to predict the hydrological functioning of rainwater harvesting systems of Dry Chaco rangelands (Table 1, Figure 3). As is known, there is a trade-off between the model fit and its simplicity. To reach an optimal solution is the great challenge of model development. Our model reached high accuracy, and, at the same time, it only needs daily rainfall and air temperature data series to be run. Thus, we consider that it can easily be used by scientists, ranchers, or local decision-makers of Dry Chaco rangelands, and it is also able to be adapted to other similar flat and dry rangelands of the world.

Monitoring and modeling time series to predict large water reservoirs and/or rivers dynamics responses to rainfall events, atmospheric conditions, and landscape alterations have been already assessed in more humid regions [48–51]. In the case of drylands, two additional challenges can be added to make the system more complex, such as the frequency of stochastic events (e.g., extreme rainfall events or flash floods) and extreme drought situations that generate the loss of all the water storage (see, for example Figures 4 and 5), or the temporary absent of flow in rivers. The model developed in this paper presented a good performance in capturing extreme events, but presented more difficulties to predict the moment and/or the last of the empty periods. We consider that more research is needed to go deeper into this second aspect. At the same time, having data from more sites may improve our knowledge of these systems in different sites in the region, or even in other regions where impoundments are the main alternative for water supply.

Most of the research applied to drought management focus on big reservoirs [52,53] or groundwater [54–56] as main sources of water supply. However, despite its great importance providing water in Dry Chaco rangelands, there is little scientific knowledge about the hydrological functioning of rainwater harvesting systems and their biophysical controls. Typically, there is one rainwater harvesting system every 1230 ha, with the cattle-grazed rangeland collecting only a tiny fraction of the rain falling in their contributory

areas [25]. Based on a large number of observations and field data, Magliano et al. [10] proposed an ecohydrological framework to explain surface water circulation in Dry Chaco rangelands. Although this framework was proposed in theoretical terms, our models provide an opportunity to test these concepts. This will allow scientists to think about the relationship between watershed characteristics and model parameter values (Table 1, Figure 3), or whether those values might be changed by cattle management. Furthermore, these models can test general hypotheses about the impacts of climate variability (e.g., a string of dry years) or changes in the structure of rainfall (e.g., less frequent but highly intense events [57]) on the hydrological functioning of rainwater harvesting systems.

Rainwater harvesting has been proposed as one of the few alternatives to solve the problem of water access and food production in drylands of the world in the last two decades [10,16,58–60]. Some authors highlight three main advantages of rainwater harvesting: (i) people solve water access locally, (ii) it is a very versatile and adaptable technology especially for low-income regions, and (iii) it is part of the cultural identity and traditions of the peoples who have practiced it since ancient times [15,16,61]. However, to solve large-scale water access problems, countries or states opt for other alternatives, such as laying aqueducts, pumping groundwater tables, or seawater desalination [28,62–64]. Although these alternatives have managed to give access to water to millions of people in the world, their development and maintenance costs are very high. Based on several experiences from different parts of the world [15,61,65,66], we believe that rainwater harvesting should be a complementary alternative to provide water to people. For this, it is necessary to develop models, such as those presented here, that allow us to make hydrological and economic predictions or provide critical information about rainwater harvesting systems of the world.

5. Conclusions

The main conclusions we obtained were:

1. Water stored in impoundments followed the seasonal dynamic of rainfall, presenting more water in the wet summer season and slowly decreasing during the dry winter season;
2. A range of rainfall thresholds of 15–33 mm were found to initiate the runoff generation process;
3. Once these thresholds were reached, impoundment water gains presented linear slopes of 19–99 m^3 of water gain per mm of rainfall;
4. The previous day's storage did not affect the water loss rate in four of the six impoundments, suggesting that evaporation plays an important role in the emptying process;
5. The developed Bayesian model has good performance and only need daily temperature and rainfall data to be run; thus, it can be useful to predict the impoundments water availability according to different rainfall scenarios, test the effects of wet-dry cycles, or evaluate the impact of global change predictions in different sites. However, it is worth mentioning that our models overestimated the number of empty days in some impoundments. It will be important to go deeper into this point in future research.
6. Although the number of impoundments analyzed in this study may be limited, the model and methodology developed here are able to be replicated and/or scaled to other regions.

Author Contributions: Conceptualization, M.J.N., P.N.M. and E.G.J.; methodology, M.J.N., P.N.M. and O.A.M.; software, M.J.N. and O.A.M.; validation, O.A.M. and M.J.N.; formal analysis, M.J.N., P.N.M. and O.A.M.; investigation, M.J.N. and P.N.M.; resources, P.N.M., F.M. and R.A.P.; field work, M.J.N., F.M., P.N.M. and R.A.P.; writing—original draft preparation, M.J.N. and P.N.M.; writing—review and editing, M.J.N., P.N.M., E.G.J., F.M., M.D.N. and O.A.M.; visualization, M.J.N., P.N.M. and O.A.M.; supervision, P.N.M. and E.G.J.; project administration, P.N.M.; funding acquisition, P.N.M. All authors have read and agreed to the published version of the manuscript.

Funding: This work was funded by National Agency for the Promotion of Research, Technological Development and Innovation (PICTs 2972-2020, 02212 and 0504-2020), the CONICET-Argentina (PIPs 11220200100716CO, 0087 and 11220200100363CO), Bunge and Born Foundation and National Ministry of Science and Technology of Argentina. San Luis Applied Maths Institute (CONICET–National University of San Luis; Argentina) provided laboratory spaces and workplaces. We used satellite imagery provided by the Planet's Education and Research program.

Data Availability Statement: The code and data to reproduce the Bayesian analysis presented in this study are openly available in https://github.com/Grupo-de-modelado-probabilista/water_storage, accessed on 24 May 2023.

Acknowledgments: We thank Guillermo Heider, Pablo Capellini, Fabian, Sergio, and Pedro for their collaboration with all related with field accesses and measurements in San Agustin (San Luis, Argentina). We appreciate the generosity and the willingness of Raul Giménez, Pablo Garay y Juan Martín Loyola for helping us and for their ideas during different stages of this study, and Fernanda Bomfim for her collaboration with the graphical design.

Conflicts of Interest: The authors declare no conflict of interest.

Appendix A

Table A1. Descriptive statistics from the rain gauges and impoundments along the three years' time series. Years (first column) are represented considering the hydrological year values (from July to June) and the yearly mean of the three consecutive years for each site, for each metric. Precipitation is represented by the total annual amount and its relative contribution between October and March, and between December and February. Number of events was calculated considering daily incomes in the rain gauges associated to each impoundment and/or incomes registered in the impoundment and its relative contribution between October and March, and between December and February. Event size was represented by the mean, the 50th and 90th percentiles, and the maximum event that took place on year. Max days dry represents the maximum number of consecutive days without rainfall events. Impoundments is represented by the empty days, as the number of days that each impoundment has no water, and the impoundment gains, as the sum of all the incomes registered in a year. The last row represents the general characterization of all the sites, as the means of all the yearly values of all the sites together, for each metric.

		Precipitation			Number of Events			Event Size (mm)				Max Days Dry	Impoundments	
	Years	Total (mm)	Oct.–Mar.	Dec.–Feb.	Total	Oct.–Mar.	Dec.–Feb.	Mean	P50	P90	Max		Empty Days	Gain (m^3)
BH	1	352	80%	50%	36	72%	50%	10	5	26	56	52	0	4354
	2	516	90%	66%	44	66%	41%	12	5	31	115	35	0	6053
	3	333	89%	55%	42	69%	36%	8	2	20	45	36	0	3314
	Mean	401	86%	57%	41	69%	42%	10	4	26	72	41	0	4574
Casa	1	299	91%	66%	35	77%	46%	9	6	19	27	70	27	3641
	2	517	93%	68%	40	83%	43%	13	7	32	101	46	113	12,688
	3	376	93%	59%	39	77%	41%	10	2	24	66	73	28	4394
	Mean	397	93%	64%	38	79%	43%	10	5	25	65	63	56	6908
Fabian	1	344	91%	71%	31	81%	42%	11	8	24	43	86	0	7179
	2	491	93%	69%	43	70%	35%	11	3	27	94	35	0	16,817
	3	373	94%	68%	40	75%	40%	9	3	22	66	49	0	5454
	Mean	403	93%	70%	38	75%	39%	11	5	24	68	57	0	9817
Miguel	1	345	91%	66%	33	79%	45%	10	6	27	55	86	0	12,325
	2	469	92%	60%	44	73%	39%	11	4	30	75	34	10	22,576
	3	289	93%	68%	46	78%	41%	6	3	14	50	30	84	10,425
	Mean	368	92%	65%	41	77%	42%	9	4	24	60	50	31	15,109
Nueva	1	308	91%	57%	28	82%	46%	11	6	23	48	85	0	6702
	2	508	92%	64%	43	70%	37%	12	5	32	115	45	0	14,277
	3	376	93%	69%	42	76%	43%	9	2	20	66	59	0	10,049
	Mean	397	92%	63%	38	76%	42%	11	5	25	76	63	0	10,343
Pedro	1	345	91%	66%	34	79%	47%	10	6	26	55	86	97	10,143
	2	469	92%	60%	44	75%	39%	11	4	30	75	35	0	17,271
	3	287	94%	68%	48	75%	38%	6	2	14	50	30	0	5178
	Mean	367	92%	65%	42	76%	41%	9	4	24	60	50	32	10,864
General		389	91%	64%	40	75%	42%	10	5	24	67	54	20	9602

References

1. D'Odorico, P.; Bhattachan, A.; Davis, K.F.; Ravi, S.; Runyan, C.W. Global Desertification: Drivers and Feedbacks. *Adv. Water Resour.* **2013**, *51*, 326–344. [CrossRef]
2. Reynolds, J.F.; Kemp, P.R.; Ogle, K.; Fernández, R.J. Modifying the 'Pulse–Reserve'Paradigm for Deserts of North America: Precipitation Pulses, Soil Water, and Plant Responses. *Oecologia* **2004**, *141*, 194–210. [CrossRef]
3. Asner, G.P.; Elmore, A.J.; Olander, L.P.; Martin, R.E.; Harris, A.T. Grazing Systems, Ecosystem Responses, and Global Change. *Annu. Rev. Environ. Resour.* **2004**, *29*, 261–299. [CrossRef]
4. Maestre, F.T.; Le Bagousse-Pinguet, Y.; Delgado-Baquerizo, M.; Eldridge, D.J.; Saiz, H.; Berdugo, M.; Gozalo, B.; Ochoa, V.; Guirado, E.; García-Gómez, M. Grazing and Ecosystem Service Delivery in Global Drylands. *Science* **2022**, *378*, 915–920. [CrossRef]
5. Fernández, P.D.; Kuemmerle, T.; Baumann, M.; Grau, H.R.; Nasca, J.A.; Radrizzani, A.; Gasparri, N.I. Understanding the Distribution of Cattle Production Systems in the South American Chaco. *J. Land Use Sci.* **2020**, *15*, 52–68. [CrossRef]
6. Loik, M.E.; Breshears, D.D.; Lauenroth, W.K.; Belnap, J. A Multi-Scale Perspective of Water Pulses in Dryland Ecosystems: Climatology and Ecohydrology of the Western USA. *Oecologia* **2004**, *141*, 269–281. [CrossRef] [PubMed]
7. Noy-Meir, I. Desert Ecosystems: Environment and Producers. *Annu. Rev. Ecol. Syst.* **1973**, *4*, 25–51. [CrossRef]
8. Adham, A.; Riksen, M.; Ouessar, M.; Ritsema, C.J. A Methodology to Assess and Evaluate Rainwater Harvesting Techniques in (Semi-) Arid Regions. *Water* **2016**, *8*, 198. [CrossRef]
9. Oweis, T.; Hachum, A. Water Harvesting for Improved Rainfed Agriculture in the Dry Environments. In *Rainfed Agriculture: Unlocking the Potential*; CABI: Wallingford, UK, 2009; pp. 164–181.
10. Magliano, P.N.; Breshears, D.D.; Murray, F.; Niborski, M.J.; Nosetto, M.D.; Zou, C.B.; Jobbágy, E.G. South American Dry Chaco Rangelands: Positive Effects of Cattle Trampling and Transit on Ecohydrological Functioning. *Ecol. Appl.* **2023**, *33*, e2800. [CrossRef]
11. Adema, E.O. Manejo de Agua, Suelo y Vegetación en Ambientes Semiáridos-áridos. Asociación Argentina de las Ciencias del Suelo. Año Internacional de los Suelos. Available online: https://inta.gob.ar/sites/default/files/script-tmp-inta-manejo_de_agua_suelo_y_vegetacin_en_ambientes_s.pdf (accessed on 19 April 2021).
12. Nicholson, S.E. *Dryland Climatology*; Cambridge University Press: Cambridge, UK, 2011; pp. 1–528.
13. Wang, L.; d'Odorico, P.; Evans, J.P.; Eldridge, D.J.; McCabe, M.F.; Caylor, K.K.; King, E.G. Dryland Ecohydrology and Climate Change: Critical Issues and Technical Advances. *Hydrol. Earth Syst. Sci.* **2012**, *16*, 2585–2603. [CrossRef]
14. Wilcox, B.P.; Sorice, M.G.; Young, M.H. Dryland Ecohydrology in the Anthropocene: Taking Stock of Human–Ecological Interactions. *Geogr. Compass* **2011**, *5*, 112–127. [CrossRef]
15. Paz-Kagan, T.; Ohana-Levi, N.; Shachak, M.; Zaady, E.; Karnieli, A. Ecosystem Effects of Integrating Human-Made Runoff-Harvesting Systems into Natural Dryland Watersheds. *J. Arid Environ.* **2017**, *147*, 133–143. [CrossRef]
16. Oweis, T.Y.; Prinz, D.; Hachum, A.Y. *Rainwater Harvesting for Agriculture in the Dry Areas*; CRC Press: Boca Raton, FL, USA, 2012.
17. Wilcox, B.P.; Breshears, D.D.; Allen, C.D. Ecohydrology of a Resource-conserving Semiarid Woodland: Effects of Scale and Disturbance. *Ecol. Monogr.* **2003**, *73*, 223–239. [CrossRef]
18. Aguilera, M.O.; Steinaker, D.F.; Demaria, M.R. Runoff and Soil Loss in Undisturbed and Roller-Seeded Shrublands of Semiarid Argentina. *J. Range Manag.* **2003**, *56*, 227–233. [CrossRef]
19. Marín-Comitre, U.; Schnabel, S.; Pulido-Fernández, M. Hydrological Characterization of Watering Ponds in Rangeland Farms in the Southwest Iberian Peninsula. *Water* **2020**, *12*, 1038. [CrossRef]
20. Magliano, P.N.; Mindham, D.; Tych, W.; Murray, F.; Nosetto, M.D.; Jobbágy, E.G.; Niborski, M.J.; Rufino, M.C.; Chappell, N.A. Hydrological Functioning of Cattle Ranching Impoundments in the Dry Chaco Rangelands of Argentina. *Hydrol. Res.* **2019**, *50*, 1596–1608. [CrossRef]
21. Duesterhaus, J.L.; Ham, J.M.; Owensby, C.E.; Murphy, J.T. Water Balance of a Stock-Watering Pond in the Flint Hills of Kansas. *Rangel. Ecol. Manag.* **2008**, *61*, 329–338. [CrossRef]
22. Magliano, P.N.; Murray, F.; Baldi, G.; Aurand, S.; Páez, R.A.; Harder, W.; Jobbágy, E.G. Rainwater Harvesting in Dry Chaco: Regional Distribution and Local Water Balance. *J. Arid Environ.* **2015**, *123*, 93–102. [CrossRef]
23. Basán Nickisch, M. *Manejo de Recursos Hídricos Para Áreas de Secano*, 2nd ed.; Ediciones Instituto Nacional de Tecnolía Agropecuaria: Buenos Aires, Argentina, 2012; pp. 1–136.
24. Umazano, A.M.; Adema, E.O.; Aimar, S.B. Tajamares: Una Tecnología Alternativa Para La Zona Árida-Semiárida de La Pampa. *INTA* **2004**, *56*, 1–56.
25. Niborski, M.J.; Murray, F.; Jobbagy Gampel, E.G.; Nosetto, M.D.; Fernandez, P.D.; Castellanos, G.; Magliano, P.N. Distribución Espacial y Controles Ambientales de Las Represas (Tajamares) En El Chaco Árido; *Ecol. Austral* **2022**, *32*, 158–173.
26. Magliano, P.N.; Fernández, R.J.; Mercau, J.L.; Jobbágy, E.G. Precipitation Event Distribution in Central Argentina: Spatial and Temporal Patterns. *Ecohydrology* **2015**, *8*, 94–104. [CrossRef]
27. Calderon, M.R.; Almeida, C.A.; Jofré, M.B.; González, S.P.; Miserendino, M.L. Flow Regulation by Dams Impacts More than Land Use on Water Quality and Benthic Communities in High-Gradient Streams in a Semi-Arid Region. *Sci. Total Environ.* **2023**, *881*, 163468. [CrossRef] [PubMed]
28. Llanes, A.L.; Poca, M.; Jimenez, Y.G.; Castellanos, G.; Gómez, B.M.; Marchese, M.; Lana, N.B.; Pascual, M.; Albariño, R.; Barral, M.P. De Dónde Viene Ya Dónde va El Agua de Las Ciudades? Base de Datos Integrada Para 243 Centros Urbanos Argentinos. *Ecol. Austral* **2022**, *32*, 1133–1149. [CrossRef]

29. Jobbágy, E.G.; Acosta, A.M.; Nosetto, M.D. Rendimiento Hídrico En Cuencas Primarias Bajo Pastizales y Plantaciones de Pino de Las Sierras de Córdoba (Argentina). *Ecol. Austral* **2013**, *23*, 87–96. [CrossRef]
30. Oyarzabal, M.; Clavijo, J.; Oakley, L.; Biganzoli, F.; Tognetti, P.; Barberis, I.; Maturo, H.M.; Aragón, R.; Campanello, P.I.; Prado, D. Unidades de Vegetación de La Argentina. *Ecol. Austral* **2018**, *28*, 40–63. [CrossRef]
31. Karlin, M.S.; Karlin, U.O.; Coirini, R.O.; Reati, G.J.; Zapata, R.M. *El Chaco Árido*; Universidad Nacional de Córdoba: Córdoba, Argentina, 2013.
32. Morello, J.; Matteucci, S. Capítulo 4: Ecorregión del Chaco Seco. In *Ecorregiones y Complejos Ecosistémicos Argentinos*, 2nd ed.; Morello, J., Matteucci, S., Rodriguez, A., Silva, M., Eds.; Orientación Gráfica Editora S.R.L.: Buenos Aires, Argentina, 2012; pp. 151–203.
33. Magliano, P.N.; Fernández, R.J.; Florio, E.L.; Murray, F.; Jobbágy, E.G. Soil Physical Changes after Conversion of Woodlands to Pastures in Dry Chaco Rangelands (Argentina). *Rangel. Ecol. Manag.* **2017**, *70*, 225–229. [CrossRef]
34. Steinaker, D.F.; Jobbágy, E.G.; Martini, J.P.; Arroyo, D.N.; Pacheco, J.L.; Marchesini, V.A. Vegetation Composition and Structure Changes Following Roller-Chopping Deforestation in Central Argentina Woodlands. *J. Arid Environ.* **2016**, *133*, 19–24. [CrossRef]
35. Blanco, L.J.; Ferrando, C.A.; Biurrun, F.N.; Oriente, E.L.; Namur, P.; Recalde, D.J.; Berone, G.D. Vegetation Responses to Roller Chopping and Buffelgrass Seeding in Argentina. *Rangel. Ecol. Manag.* **2005**, *58*, 219–224. [CrossRef]
36. Kumar, M.D.; Ghosh, S.; Patel, A.; Singh, O.P.; Ravindranath, R. Rainwater Harvesting in India: Some Critical Issues for Basin Planning and Research. *Land Use Water Resour. Res.* **2006**, *6*, 1–17.
37. Pilgrim, D.H.; Chapman, T.G.; Doran, D.G. Problems of Rainfall-Runoff Modelling in Arid and Semiarid Regions. *Hydrol. Sci. J.* **1988**, *33*, 379–400. [CrossRef]
38. Ngigi, S.N.; Savenije, H.H.; Gichuki, F.N. Land Use Changes and Hydrological Impacts Related to Up-Scaling of Rainwater Harvesting and Management in Upper Ewaso Ng'iro River Basin, Kenya. *Land Use Policy* **2007**, *24*, 129–140. [CrossRef]
39. Ceballos, A.; Schnabel, S. Hydrological Behaviour of a Small Catchment in the Dehesa Landuse System (Extremadura, SW Spain). *J. Hydrol.* **1998**, *210*, 146–160. [CrossRef]
40. Wiecki, T.; Salvatier, J.; Vieira, R.; Kochurov, M.; Patil, A.; Osthege, M.; Willard, B.T.; Engels, B.; Carroll, C.; Martin, O.A.; et al. Pymc-Devs/Pymc: V5.3.1. 2023. Available online: https://zenodo.org/record/7868623 (accessed on 10 March 2023).
41. Salvatier, J.; Wiecki, T.V.; Fonnesbeck, C. Probabilistic Programming in Python Using PyMC3. *PeerJ Comput. Sci.* **2016**, *2*, e55. [CrossRef]
42. Kumar, R.; Carroll, C.; Hartikainen, A.; Martín, O.A. ArviZ a Unified Library for Exploratory Analysis of Bayesian Models in Python. *J. Open Source Software.* **2019**, *4*, 1143. [CrossRef]
43. Martin, O.A.; Teste, F.P. A Call for Changing Data Analysis Practices: From Philosophy and Comprehensive Reporting to Modeling Approaches and Back. *Plant Soil* **2022**, *476*, 743–753. [CrossRef]
44. Martin, O.A.; Kumar, R.; Lao, J. *Bayesian Modeling and Computation in Python*; CRC Press: Boca Raton, FL, USA, 2021.
45. Gelman, A.; Vehtari, A.; Simpson, D.; Margossian, C.C.; Carpenter, B.; Yao, Y.; Kennedy, L.; Gabry, J.; Bürkner, P.-C.; Modrák, M. Bayesian Workflow. *arXiv* **2020**, arXiv:2011.01808.
46. Gabry, J.; Simpson, D.; Vehtari, A.; Betancourt, M.; Gelman, A. Visualization in Bayesian Workflow. *J. R. Stat. Soc. Ser. A Stat. Soc.* **2019**, *182*, 389–402. [CrossRef]
47. Abatzoglou, J.T.; Dobrowski, S.Z.; Parks, S.A.; Hegewisch, K.C. TerraClimate, a High-Resolution Global Dataset of Monthly Climate and Climatic Water Balance from 1958–2015. *Sci. Data* **2018**, *5*, 1–12. [CrossRef]
48. Wagener, T.; Dadson, S.J.; Hannah, D.M.; Coxon, G.; Beven, K.; Bloomfield, J.P.; Buytaert, W.; Cloke, H.; Bates, P.; Holden, J. Knowledge Gaps in Our Perceptual Model of Great Britain's Hydrology. *Hydrol. Process.* **2021**, *35*, e14288. [CrossRef]
49. Wohl, E.; Barros, A.; Brunsell, N.; Chappell, N.A.; Coe, M.; Giambelluca, T.; Goldsmith, S.; Harmon, R.; Hendrickx, J.M.; Juvik, J. The Hydrology of the Humid Tropics. *Nat. Clim. Chang.* **2012**, *2*, 655–662. [CrossRef]
50. Chappell, N.A.; Franks, S.W.; Larenus, J. Multi-scale Permeability Estimation for a Tropical Catchment. *Hydrol. Process.* **1998**, *12*, 1507–1523. [CrossRef]
51. Beven, K.J. *Rainfall-Runoff Modelling: The Primer*; John Wiley & Sons: Hoboken, NJ, USA, 2011.
52. Rubio-Martin, A.; Pulido-Velazquez, M.; Macian-Sorribes, H.; Garcia-Prats, A. System Dynamics Modeling for Supporting Drought-Oriented Management of the Jucar River System, Spain. *Water* **2020**, *12*, 1407. [CrossRef]
53. Perrin, J.; Ferrant, S.; Massuel, S.; Dewandel, B.; Maréchal, J.-C.; Aulong, S.; Ahmed, S. Assessing Water Availability in a Semi-Arid Watershed of Southern India Using a Semi-Distributed Model. *J. Hydrol.* **2012**, *460*, 143–155. [CrossRef]
54. Bakker, M.; Schaars, F. Solving Groundwater Flow Problems with Time Series Analysis: You May Not Even Need Another Model. *Groundwater* **2019**, *57*, 826–833. [CrossRef]
55. Fan, Y. Groundwater in the E Arth's Critical Zone: Relevance to Large-scale Patterns and Processes. *Water Resour. Res.* **2015**, *51*, 3052–3069. [CrossRef]
56. Scanlon, B.R.; Keese, K.E.; Flint, A.L.; Flint, L.E.; Gaye, C.B.; Edmunds, W.M.; Simmers, I. Global Synthesis of Groundwater Recharge in Semiarid and Arid Regions. *Hydrol. Process. Int. J.* **2006**, *20*, 3335–3370. [CrossRef]
57. Stocker, T. *Climate Change 2013: The Physical Science Basis: Working Group I Contribution to the Fifth Assessment Report of the Intergovernmental Panel on Climate Change*; Cambridge University Press: Cambridge, UK, 2014.
58. Zhu, Q.; Gould, J.; Li, Y.; Ma, C. *Rainwater Harvesting for Agriculture and Water Supply*; Springer: Berlin/Heidelberg, Germany, 2015.

59. Falkenmark, M.; Fox, P.; Persson, G.; Rockström, J. Water Harvesting for Upgrading of Rainfed Agriculture. *Probl. Anal. Res. Needs* **2001**, *11*, 76–87.
60. Bruins, H.J.; Evenari, M.; Nessler, U. Rainwater-Harvesting Agriculture for Food Production in Arid Zones: The Challenge of the African Famine. *Appl. Geogr.* **1986**, *6*, 13–32. [CrossRef]
61. Adham, A.; Riksen, M.; Ouessar, M.; Abed, R.; Ritsema, C. Development of Methodology for Existing Rainwater Harvesting Assessment in (Semi-) Arid Regions. In *Water and Land Security in Drylands: Response to Climate Change*; Springer: Cham Switzerland, 2017; pp. 171–184.
62. Huggins, X.; Gleeson, T.; Kummu, M.; Zipper, S.C.; Wada, Y.; Troy, T.J.; Famiglietti, J.S. Hotspots for Social and Ecological Impacts from Freshwater Stress and Storage Loss. *Nat. Commun.* **2022**, *13*, 439. [CrossRef]
63. Jobbágy, E.G.; Pascual, M.; Barral, M.P.; Poca, M.; Silva, L.G.; Oddi, J.; Castellanos, G.; Clavijo, A.; Díaz, B.G.; Villagra, P.E. Representación Espacial de La Oferta y La Demanda de Los Servicios Ecosistémicos Vinculados al Agua. *Ecol. Austral* **2022**, *32*, 213–228. [CrossRef]
64. Trimble, M.; Olivier, T.; Anjos, L.A.; Dias Tadeu, N.; Giordano, G.; Mac Donnell, L.; Laura, R.; Salvadores, F.; Santana-Chaves, I.M.; Torres, P.H. How Do Basin Committees Deal with Water Crises? Reflections for Adaptive Water Governance from South America. *Ecol. Soc.* **2022**, *27*, 42. [CrossRef]
65. Lo, A.G.; Gould, J. Rainwater Harvesting: Global Overview. In *Rainwater Harvesting for Agriculture and Water Supply*; Springer Singapore and Science Press: Beijing, China, 2015; pp. 213–233.
66. Ali, A.; Oweis, T.; Rashid, M.; El-Naggar, S.; Aal, A.A. Water Harvesting Options in the Drylands at Different Spatial Scales. *Land Use Water Resour. Res.* **2007**, *7*, 1–13.